



# Humidity-responsive actuation of programmable hydrogel microstructures based on 3D printing

Chao Lv<sup>a</sup>, Xiang-Chao Sun<sup>a</sup>, Hong Xia<sup>a,\*</sup>, Yan-Hao Yu<sup>a</sup>, Gong Wang<sup>a</sup>, Xiao-Wen Cao<sup>b</sup>, Shun-Xin Li<sup>a</sup>, Ying-Shuai Wang<sup>a</sup>, Qi-Dai Chen<sup>a</sup>, Yu-De Yu<sup>c</sup>, Hong-Bo Sun<sup>a,d,\*</sup>

<sup>a</sup> State Key Laboratory of Integrated Optoelectronics, College of Electronic Science and Engineering, Jilin University, 2699 Qianjin Street, Changchun 130012, China

<sup>b</sup> School of Mechanical Science and Engineering, Jilin University, 5988 Renmin Street, Changchun 130025, China

<sup>c</sup> State Key Laboratory of Integrated Optoelectronics, Institute of Semiconductors, Chinese Academy of Sciences, Beijing 100083, China

<sup>d</sup> State Key Lab of Precision Measurement and Instruments, Department of Precision Instrument, Tsinghua University, Haidian, Beijing 100084, China

## ARTICLE INFO

### Article history:

Received 11 July 2017

Received in revised form

14 November 2017

Accepted 11 December 2017

Available online 15 December 2017

### Keywords:

Programmable hydrogel microstructures

Humidity-responsive

Actuation

3D printing

## ABSTRACT

The design and fabrication of devices that based on adaptive soft matter with the autonomous transduction of environmental and field signals is an interesting area of material science and device engineering. Additive manufacturing, also known as 3D printing, has gained great attention as it allows the creation of complex 3D geometries with precisely prescribed microarchitectures, which enable new functionalities or improved performance. Here, we report on poly(ethylene glycol) diacrylate hydrogel microstructures with excellent humidity responsiveness by 3D printing of two-photon photopolymerization. The voxels of fabricated hydrogel microstructures have controllable crosslinking density because adjusting fabrication parameters, therefore controllable humidity-driven swelling ability can be achieved. Using the proper parameters, we present an array of microstructures which can realize the function of nano-interconnected network and a hydrogel microstructure with pores to mimic the open and close of the stomata of plants. Based on a flexible two-steps fabrication method and the combination of active and inert materials, binary encoding micropillar arrays and joint-like cantilever microstructure have been easily fabricated. The humidity-responsive actuation of hydrogel microstructures is repeatable and stable over 10000 cycles. This kind of composite hydrogel microstructures may lead to great promise for the diverse applications such as sensors, actuators or construction of soft robots.

© 2017 Elsevier B.V. All rights reserved.

## 1. Introduction

In recent years, the design and fabrication of devices that based on adaptive soft matter with the autonomous transduction of environmental and field signals is an interesting area of material science and device engineering. Development of micro/nanoresolution three-dimensional (3D) fabrication of the smart materials is still necessary to expand the utility of these materials across a broader range of applications. The adaptive hydrogel materials are being actively researched due to their importance in artificial muscles [1], molecular motors [2], soft robotics [3–5], programmable origami [6–8] and energy generators [9,10]. Mechanical movement of the hydrogel exhibits reversible shape changes in response to environmental stimuli, such as light [11–13], thermal [14], electrical [15] or chemical energy [16]. According to the stimuli, responsive hydrogels could provide an alternative means to control precise

microscopic motions, potentially through the action of multiple, or independent components functioning. Moisture-triggered movement of hydrogel have recently been developed, which are independent of chemical, electrical, and other critical triggers [17–21]. Certain hydrogel, like film combining both (polypyrrole) and (polyol-borate), could be as generator by associating this film with a piezoelectric element, which driven by water gradients to outputs alternating electricity [22]. Such an energy harvesting technology, which makes use of energy gaps temporarily generated under ambient conditions for operating small mechanical devices on the spot, it is now recognized as very important for realizing a sustainable society.

The ubiquitous presence of humidity in ambient air and its variation makes the development of humidity-responsive movement both appealing and of importance. By chance, the capability to convert simple environmental stimuli, such as humidity, into mechanical reversible motion is regularly observed in living systems, particularly plants [23]. These systems are capable of converting the sorption and desorption of water into driving forces for movement. A well-known example is the release of ripe seeds

\* Corresponding authors.

E-mail addresses: [hxia@jlu.edu.cn](mailto:hxia@jlu.edu.cn) (H. Xia), [hbsun@tsinghua.edu.cn](mailto:hbsun@tsinghua.edu.cn) (H.-B. Sun).

from pine cones, which open due to a bending movement of their scales during drying in ambient air and close in wet conditions [24]. Similarly, seeds from wild wheat are propelled into soil after being released, which is solely due to the daily change in humidity that induces a curvature of the awns depending on the moisture level [25]. Stomatal pores are located on the plant epidermis and regulate CO<sub>2</sub> uptake for photosynthesis and water loss to drive transpiration. Stomatal movement is induced by several environmental factors, including air humidity [26]. When the humidity is high, the leaf epidermal cells have large volume due to containing high water content, and squeeze the guard cell, leading to stomatal closing. A stomata-inspired membrane with humidity-responsive variation of morphology has strong potential for various engineering applications in the future [27,28].

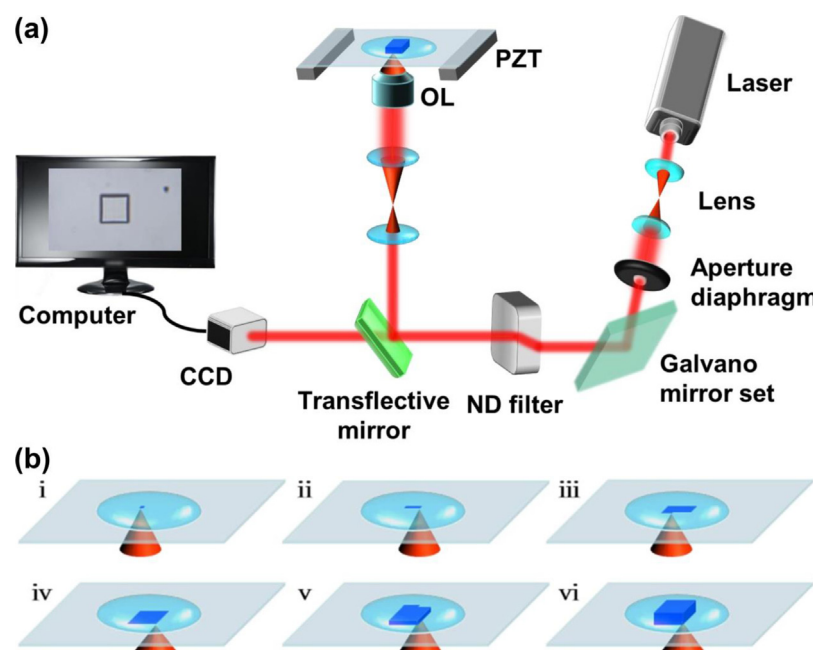
Synthetic routes and fabrication strategies leading to new-generation, dynamically tunable devices that show adaptive responses, for example, stimuli-responsive pumps, and optics valves from hydrogel in microchannel [29,30]. To the best of our knowledge, most of the researches focused on the response movement of hydrogel macrostructure, only a few works have investigated the responsiveness of the 3D hydrogel microstructures, the micro- and nano-scale 3D hydrogel structures with high-resolution topographic control will serve as smart devices for broad application [31–34], one reason is that there is still a challenge of the controllable 3D fabrication of the responsive hydrogel microstructure. As a designable three-dimensional micro-nanoprocessing method, 3D printing based on two-photon photopolymerization (TPP) of photopolymers provides an efficient route for fabricating micro-nanomachines with higher spatial resolution and smaller size [35–41]. In the 3D printing technology, femtosecond laser direct writing (FsLDW) is a point-by-point scanning method, the laser beam is focused and scanned according to the designed patterns point by point, then from the bottom slice to the upside slice until achieve the entire 3D structure. The fabricated microstructures are consisted of a number of voxels, and the crosslinking density of the voxels is controllable by changing the fabrication parameters. For hydrogels, the responsiveness and the swelling ability are related to the crosslinking density of the hydrogel network, a relatively lower crosslinking density is beneficial to

improve the swelling ability of hydrogel materials [42,43]. If the crosslinking density of the hydrogel can be controlled, the hydrogel structures with different swelling ability can be prepared. So the 3D printing method was expected to prepare hydrogel microstructures with fine morphology and excellent responsiveness, and by changing the processing conditions, the voxel crosslinking density of the polymer could be adjusted, further affect the responsiveness of the fabricated microstructures. Here, we demonstrate the humidity-driven movement of poly(ethylene glycol) diacrylate (PEG-DA) hydrogel microstructures by FsLDW. By changing the fabricating parameters, the crosslinking density of the voxels was controllable to achieve different function such as the nano-interconnection. A two-steps fabrication method was presented to combine the active and inert materials to demonstrate the application diversity of the PEG-DA hydrogel microstructures.

## 2. Experiments

### 2.1. Fabrication of PEG-DA microstructures

The PEG-DA (average M<sub>n</sub> 700), methylene blue (MB) were purchased from Sigma-Aldrich and used without further purification. MB as photoinitiator was dissolved in deionized water with the concentration of 3 mg mL<sup>-1</sup>. Then add 30 μL of the MB aqueous solution into 100 μL of PEG-DA monomer and the mixture was sonicated in dark for 5 min to assure sufficient dissolution of all the chemicals and used immediately. The PEG-DA microstructures were fabricated on coverslips using a home-made FsLDW system. The femtosecond laser beam (Spectra Physics MTEV VF-N1S, 80 MHz repetition rate, 100 fs pulse width, 800 nm central wavelength) was tightly focused in the hydrogel prepolymer solution by using a 60 × oil immersion objective lens with a high-numerical-aperture (Olympus, NA = 1.40). A piezo stage (Physik Instrumente P-622.ZCD) and a two-galvo-mirror set was used to control the vertical and horizontal scanning movements of the focused laser spot simultaneously. A charge-coupled device was used to observe the fabricating process in real time (**Scheme 1a**). During the fabrication, in order to minimize the effect of solution evaporation, a small chamber of PDMS was used to cover the prepolymer solu-



**Scheme 1.** Schematic illustration of (a) the FsLDW fabrication of hydrogel microstructures and (b) point-by-point scanning process.

tion. For various 3D microstructures, the computer program was firstly designed by 3Ds Max and converted to computer processing data and then controlled the 3D scanning of FsLDW. According to the computer processing data, the laser focal spot scanned laterally at a certain height by steering the two-galvano-mirror set, and when the scanning point-by-point in this horizontal plane was finished, the piezoelectric stage controlled the sample to move along the optical axis, repeated this process until the entire structure was fabricated ([Scheme 1b](#)). After fabrication, the sample was rinsed in the mixture of ethanol and deionized water with volume ratio of 1:2 several times to remove the unpolymerized prepolymer solution, the PEG-DA microstructures were obtained on the coverslip.

## 2.2. Fabrication of micropillar array

We first fabricated methacrylate-based micropillars by FsLDW, the methacrylate-based photoresist consisted of 36 wt% butyl methacrylate (BMA), 56 wt% propoxylated trimethylolpropane tri-acrylate, 4 wt% 2,4,6-trimethylbenzoyldiphenyl phosphine oxide and 4 wt% phenylbis(2,4,6-trimethylbenzoyl) phosphine oxide. The BMA micropillars were fabricated at the special position and after fabrication the sample was rinsed in ethanol to remove the unpolymerized solution and dried in the air. Then we dropped the PEG-DA prepolymer solution on the sample and fabricated the PEG-DA micropillars. After developing in water and drying in the air, the micropillar array with pre-stored information was obtained.

## 2.3. Characterization

The optical micrographs were taken by a Motic BA400 microscope and a charge-coupled device. A commercial humidifier with 3 mm diameter nozzle was used to applying the water vapor. When the nozzle approached the sample, the relative humidity (RH) around the sample increased and the PEG-DA microstructure swelled. The distance between the nozzle and the sample was about 3 cm, and the RH around the sample would increase to 100% when the water vapor applied for about 4 s. When removed the nozzle, the RH around the sample quickly decrease to the environment humidity (RH of 20%), the PEG-DA microstructure deswelled to the original volume. During the measurement, the room temperature was  $20 \pm 0.5^\circ\text{C}$ . The fluorescent microscope images of PEG-DA microstructures were taken using a fluorescence microscope equipped with a sub-565-nm filtering slice to filter 532-nm pumping laser light out (UB203i, Chongqing UOP Photoelectric Technology Co., Ltd., China). The morphologies of the PEG-DA hydrogel microstructures were characterized by using a field emission scanning electron microscope (Philips XL-30 ESEM). A thin layer of Au was sputtered onto the sample for better SEM imaging.

## 3. Results and discussion

PEG-DA is a kind of widely used material which have found widespread applications as biomaterials because of the particularly biocompatibility. Due to its ability to form hydrogen bonds between the PEG chains and water molecule in the humid environment, PEG-DA shows a high humidity sorption property. The PEG-DA monomer can be easily photopolymerization by FsLDW when the presence of MB as photosensitizer. After fabrication, the sample was rinsed in water several times to remove the unpolymerized prepolymer solution and then the sample was dried in the air, the preprogrammed true 3D microstructures were obtained. Owing to the advantages of 3D printing, the fabricated PEG-DA microstructures have fine morphology qualities, and the networks of the microstructures were compact, the volumes and geometries were the same as designed. When we immersed the microstructures into water or RH around the PEG-DA microstructure increased, the

water molecules diffused into the molecule network of the PEG-DA microstructure and the microstructures swelled ([Fig. 1a](#)). A flower-shaped PEG-DA microstructure was fabricated, the flower was complete and the diameter of the flower was about 35  $\mu\text{m}$  as designed ([Fig. 1b](#)). When the flower was immersed into water, it absorbed water and the size of the flower became larger significantly within seconds ([Fig. 1c](#)). After absorbing water, the diameter of the flower was about 54  $\mu\text{m}$ , the flower swelled to about 155%. The flower shrank back to the original size after the sample was picked up from water and this process can be repeated many times without damage. Besides putting the sample into water directly, the flower could swell by applying water vapor on it, it absorbed water vapor and swelled quickly, and when the water vapor was off, the flower would return to its original size fast ([Movie S1, Supporting Information](#)). The swelling and deswelling processes were repeated for 10000 cycles ([Fig. S1-2, Supporting Information](#)), the diameter swelling ratios of the microstructure fluctuated around 120% under the applying of water vapor, the difference between the maximum swelling diameter ratio and the minimum swelling diameter ratio was 7%. When the water vapor was off, the flower-shaped microstructure deswelled and returned to their original volume, showed that the PEG-DA hydrogel microstructures have good swelling stability during the swelling and deswelling process under humidity driving.

The swelling ability of the PEG-DA microstructure was related to the crosslinking density of hydrogel voxels, which could be adjusted by changing the fabricating parameters during the FsLDW process. The laser beam was tightly focused into a small point by using an objective lens with high numerical aperture, inducing the photopolymerization of hydrogel material near the focus spot to form a voxel. In order to adjust the voxel crosslinking density of the fabricated microstructures, we can change the distance between two voxels by modifying the computer programs, namely the laser scanning step length, or if we fixed the laser scanning step length, change the size of the voxel, the crosslinking density was also different ([Fig. S3, Supporting Information](#)). In order to investigate the dependence of fabricating parameters during the FsLDW on the swelling ability of the PEG-DA hydrogel microstructure, cuboid microstructures with size of  $10 \mu\text{m} \times 8 \mu\text{m} \times 1 \mu\text{m}$  were fabricated under different conditions to evaluate the swelling abilities. The cuboid microstructures were elevated on four cylindrical pedestals (1.5  $\mu\text{m}$  in diameter, 6.5  $\mu\text{m}$  in height) because this is conducive to swelling. The areas of the microstructures in the air ( $S_0$ ) and in water ( $S$ ) were measured and the area swelling ratios ( $S/S_0$ ) was calculated to evaluate the swelling abilities. First, we fixed the layer distance at 100 nm and adjusted the point distance in x-y plane from 50 nm to 250 nm (the average laser power density was about  $13 \text{ mW } \mu\text{m}^{-2}$ ), we can see that the swelling ratio increase from about 1.14–1.4 with the point distance increased ([Fig. 1d](#)). Then we let the point distance in x-y plane constant as 100 nm, and [Fig. 1e](#) showed that the swelling ratio increased gradually as the layer distance became larger (from about 1.12–1.42). This was because that a larger scanning step length results in lower voxel crosslinking density of the PEG-DA networks, and the loose network was much easier for the water molecules to penetrate into the PEG-DA three-dimensional networks, so the swelling abilities of the fabricated microstructures were better [[44](#)]. If we increased the point distance or the layer distance beyond 250 nm, the swelling ratios would increase significantly, but the conformational integrity of the PEG-DA hydrogel microstructures may be destroyed, so in the following experiment, we chose the point distance of 200 nm and the layer distance from 100 nm to 200 nm during the fabrication, which could ensure both the structural morphology and the expansion effect of the PEG-DA hydrogel microstructures.

Besides the laser scanning step length, we can also adjust the swelling ability of the microstructures by using different laser

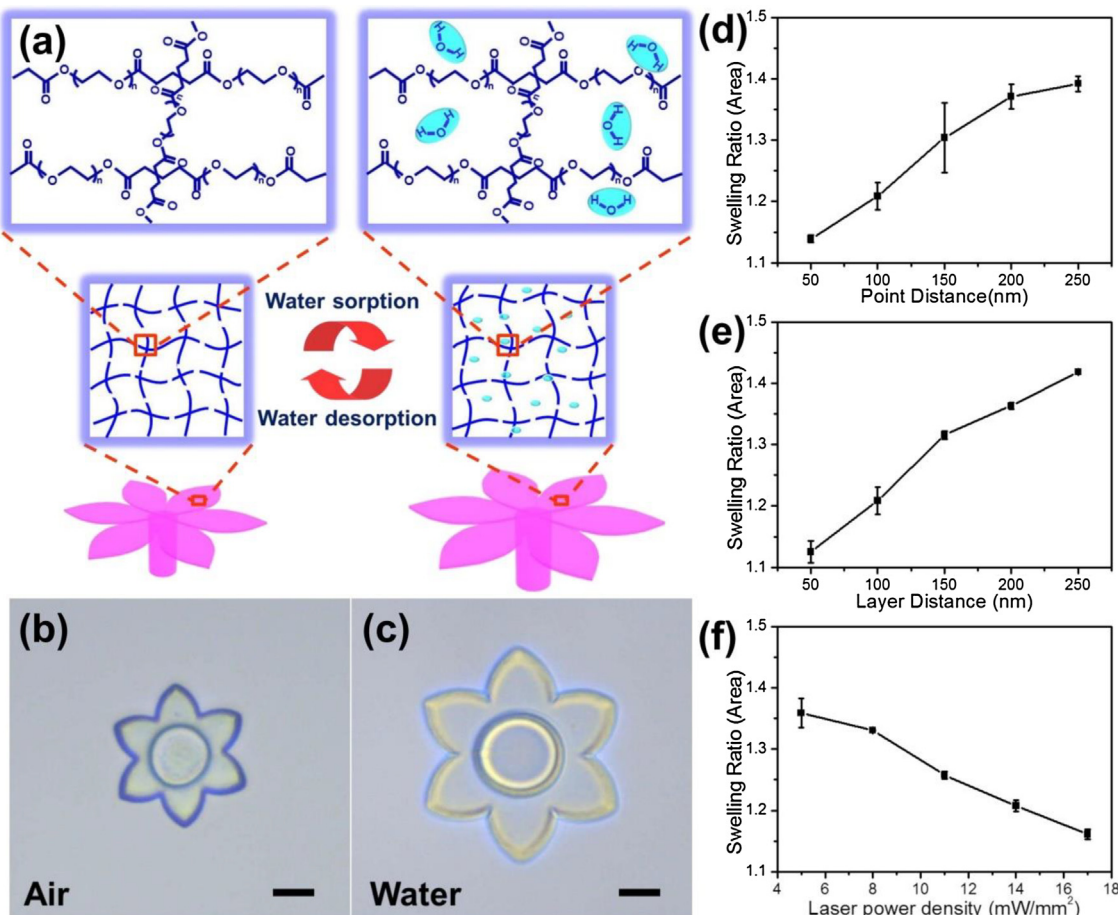


**Fig. 1.** (a) Schematic of the swelling process of the PEG-DA hydrogel microstructure fabricated by FsLDW. Optical images of the flower-shaped PEG-DA hydrogel microstructure (b) in the air and (c) in water. Scale bar: 10  $\mu\text{m}$ . Dependent curve of the area swelling ratios on (d) the point distance, (e) the layer distance and (f) the laser power density during FsLDW.

power density. When the scanning step length was fixed as 100 nm, if the laser power density was higher, the voxel became larger, resulted in a higher crosslinking density of the microstructure, and the swelling abilities of the microstructure decreased (Fig. S3d, Supporting Information). We changed the average laser power density from  $5 \text{ mW } \mu\text{m}^{-2}$  to  $17 \text{ mW } \mu\text{m}^{-2}$ , the swelling ratio of the microstructures decreased from 1.36 to 1.16 (Fig. 1f), the average laser power density of  $6.5 \text{ mW } \mu\text{m}^{-2}$  was chosen to fabricate various PEG-DA hydrogel microstructures.

Controllable hydrogel nano-interconnected network consists of several independent micro/nanostructures which were discrete after fabrication, and could connect to each other as a whole structure when triggered by a specific stimulus. This kind of hydrogel nano-interconnected network has potential applications in the fields of controlled particle transport, nano-interconnection and controllable switch. In order to achieve the function of the nano-interconnected network, the processing conditions during FsLDW should be adjusted accurately to obtain a proper swelling ratio of the PEG-DA microstructures. For PEG-DA nano-interconnected network, the proper processing conditions must ensure that when the microstructures swelled under water vapor, they could connect to each other well. If the swelling ratio of the single microstructure was too low, the swell was not enough to cause the microstructures to connect, or if the swelling ratio of the single microstructure was too high, the excessive swell of the microstructures causes the extrusion and deformation. The processing conditions used here were that 200 nm of point distance, 100 nm of layer distance and  $6.5 \text{ mW } \mu\text{m}^{-2}$  of the laser power density, we fabricated periodic

array consist of three-petaled flower microstructures. Parallelogram array and triangular array were fabricated and the radius of each three-petaled flower was  $10 \mu\text{m}$  and elevated on a  $10 \mu\text{m}$  high cylindrical pedestals, the distance between adjacent petals was  $5 \mu\text{m}$ . After fabrication, the petals of adjacent flowers did not contact each other, all flowers in the array had the same size and good morphology, there was no obvious defect from the SEM images (Fig. 2a–c; Fig. S4, Supporting Information). When we applied water vapor on it, the RH around the array increased, all three-petaled flower swelled, the petals of flowers became larger and this resulted in that a petal would contact other petals from the adjacent flowers (Fig. 2e–f, i–j; Movie S2, Supporting Information). We also observed the periodic flower array using fluorescent microscope, under the illumination of 532 nm, the array emitted bright red light because the presence of MB dye (Fig. 2g–h, k–l; Movie S3, Supporting Information). Square array consist of four-petaled flower microstructures was fabricated either and the same phenomenon was observed (Fig. 2m–p; the radius of a single flower was  $20 \mu\text{m}$  and the distance between adjacent petals was  $10 \mu\text{m}$ ). The humidity-driven nano-interconnected networks were repeatable, when the RH around the network decreased, the flower-shaped microstructures deswelled to their initial size and the petals disconnected, and this process completed in several seconds (Fig. S5–6, Supporting Information). In addition, the stability of the humidity-driven nano-interconnected networks was excellent during an observation period of 28 days (Fig. S7, Supporting Information), the swelling time and deswelling time were stable at 3–4 s. The humidity-driven nano-interconnected network

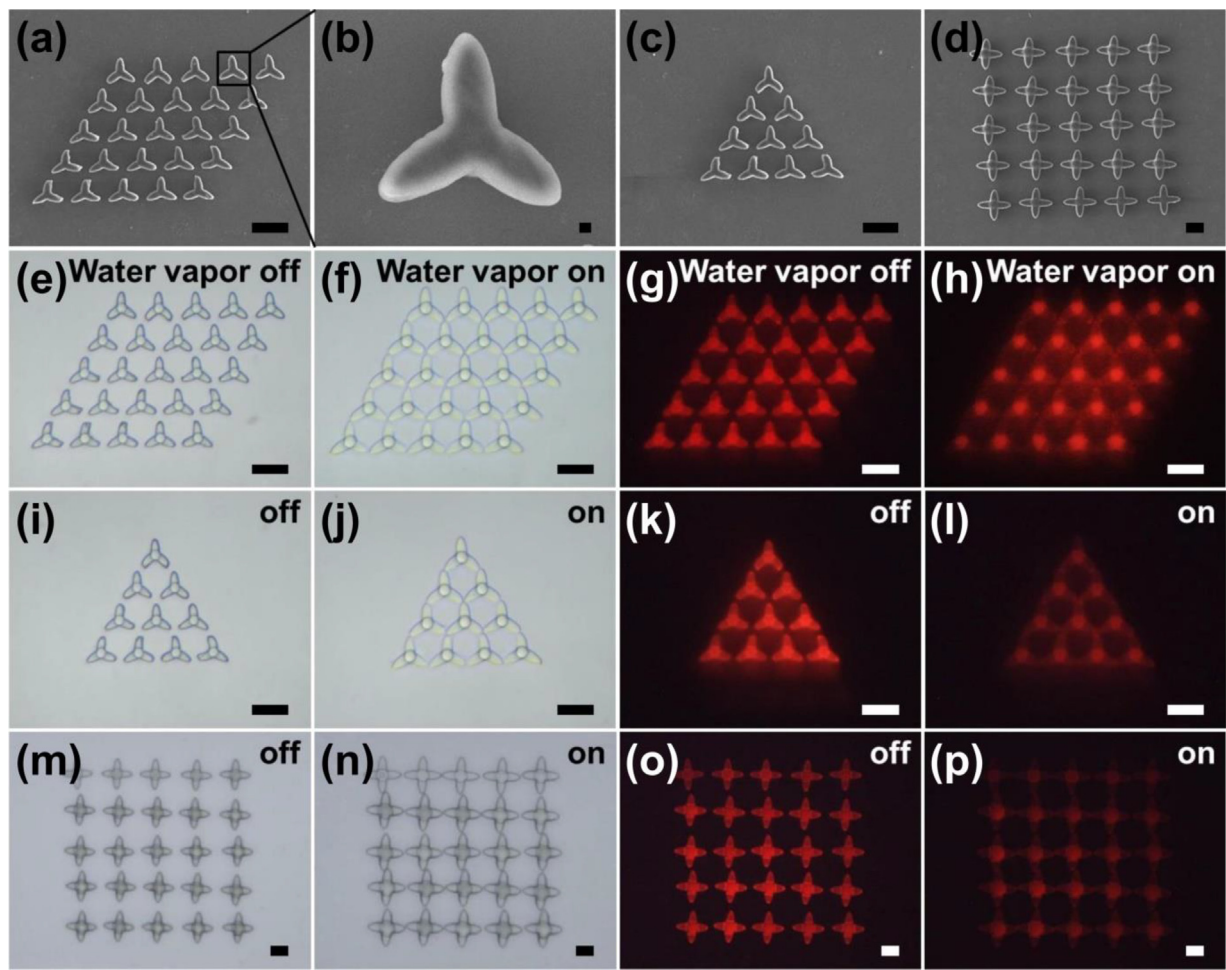


**Fig. 2.** (a) SEM image of PEG-DA hydrogel parallelogram array consist of three-petaled flower microstructures. Scale bar: 20  $\mu\text{m}$ . (b) Magnified SEM images of the single three-petaled flower microstructure in the periodic array. Scale bar: 1  $\mu\text{m}$ . SEM image of (c) triangular array consists of three-petaled flower microstructures and (d) square array consists of four-petaled flower microstructures. Scale bar: 20  $\mu\text{m}$ . (e)–(p) Optical microscope images and fluorescent microscope images of periodic array before and after the driving of water vapor. (e)–(h) Parallelogram array consists of three-petaled flower microstructures. (i)–(l) Triangular array consists of three-petaled flower microstructures. (m)–(p) Square array consists of four-petaled flower microstructures. Scale bar: 20  $\mu\text{m}$ . Conditions:  $T = 20 \pm 0.5^\circ\text{C}$ , RH  $\approx 20\%$  when water vapor was off and RH  $\approx 100\%$  when water vapor was on.

may be of importance as a controllable electrode or controllable switch, when we introduced some metal nanomaterial into the polymer microstructures, the discrete structure can form a conductive whole structure and the circuit is switched on under humid environment, and restored to off state in a dry environment.

Stomata on the leaf surface can open and close to control the exchange between plants and the environment, according to the function of stomata, a lot of controllable structures have been designed to simulate the opening or closing of stomata and widely used from separations to sensing. PEG-DA hydrogel microstructures with some stomata-like pores were fabricated using FsLDW, which have the ability to mimic the open or close of stomata. When the RH around the microstructure increased, the interval part between the adjacent stomata swelled, squeezed the stomata to become smaller or even closed. In order to let the stomata close completely, we need the interval part swell sufficiently and a large swelling ratio was necessary, so the optimized conditions used during the fabrication were 200 nm of point distance, 200 nm of layer distance and 6.5 mW  $\mu\text{m}^{-2}$  of the laser power density. The stomata could be designed into various shapes such as rhombus-shape and crescent-shape (Fig. 3). SEM images showed that all the stomata at different locations of the microstructure had the same morphology and shape as designed (Fig. 3a, d and g). From the magnified SEM images we can see that at the edge of the microstructure,

there were obvious laminar structures (Fig. S8, Supporting Information). This was because the layer distance during the fabrication was large as 200 nm, leading to a poorer interlayer connection, when the layer distance was smaller as 100 nm for the flower-shaped microstructure, no laminar structure could be observed (Fig. 2b; Fig. S4d, Supporting Information). The stomata of the fabricated hydrogel microstructures were open after fabrication and closed quickly when the surrounding RH increased, they would return to their original shape after deswelling (Movie S4; Fig. S9, Supporting Information). And even after storage in the air for more than 10 months, the humidity responsiveness of the microstructure was good, the pores still can close completely under the applying of water vapor (Fig. S10, Supporting Information). From the optical microscope images, we saw that the closure degree of the stomata in the middle of the microstructure was higher than the closure degree of the stomata at the edge of whole microstructure (Fig. 3c, f and i). This was because the stomata in the middle of the microstructure were under the squeezing from all directions and when the size of the stomata and the distance between the adjacent stomata were appropriate, the stomata could be closed completely. But for the stomata at the edge of the microstructure, the squeeze from the edge was small, so the deformations of the stoma in these directions were not enough to make the stoma completely closed.

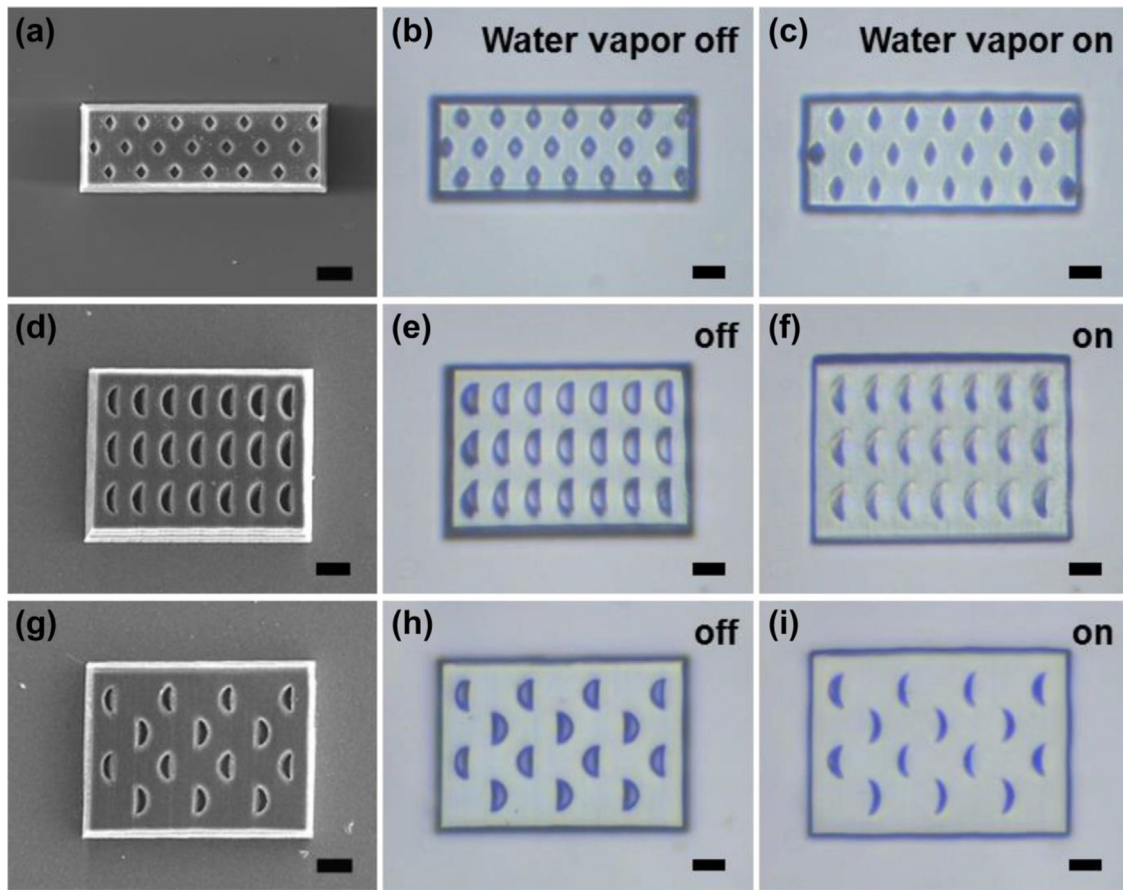


**Fig. 3.** The stomata-like hydrogel microstructures with various shaped stomata were successfully fabricated. (a) SEM image of hydrogel microstructure with rhombus-shaped stomata. (b)–(c) The open and close of rhombus-shaped stomata under the driven of water vapor. (d)–(i) The SEM images and optical microscope images of microstructures with crescent-shaped stomata. The stomata would close when the water vapor was on and open when the water vapor was off. Scale bar: 10  $\mu\text{m}$ . Conditions:  $T = 20 \pm 0.5^\circ\text{C}$ , RH  $\approx 20\%$  when water vapor was off and RH  $\approx 100\%$  when water vapor was on.

Besides the controllable crosslinking density of voxels, the FsLDW has another advantage that it could flexible integration of different materials through multi-steps femtosecond laser processing. Here, combining the active PEG-DA hydrogel materials and the inert methacrylate-based materials, a simple micropillar array was designed as binary codes for information encryption storage. Information storage is of great significance in the development of human society, due to the advantages of fast access and large amount of data storage, computers have become the most important means of information storage in recent decades, and all kinds of information are stored in computer as binary codes. Sometimes for security reasons, the stored information may need to be encrypted. The preparation procedure of the micropillar array for information encryption storage had two steps: one was the fabrication of inert methacrylate-based micropillars with no humidity response property at the special position by FsLDW, the volume of these micropillars would not change under the applying of water vapor and can be represented as "0"; then active PEG-DA hydrogel micropillars with the same size were fabricated at the other special position, under the applying of water vapor the PEG-DA micropillars swelled and represented as "1" (Fig. 4a; Fig. S11, Supporting Information). Using this method, a single letter could be presented by the eight-bit codes according to the ASCII (American Standard Code for Information Interchange) [45]. The radius of a single micropillar was 3  $\mu\text{m}$ , the height was about 4  $\mu\text{m}$  and the interval between two micropillars was 6  $\mu\text{m}$ . Because the difference between the refractive indexes of PEG-DA and the methacrylate-based material was very small, the two kinds of micropillars look

the same in the air from the optical images (Fig. 4c), when we put the micropillar array into water or applied water vapor on it, the PEG-DA hydrogel micropillars swelled and the methacrylate-based micropillars maintained their initial size, so the eight-bit codes of "01000011" were presented and demodulated as letter "C", other letters can be pre-stored into a micropillar array and read by increasing the RH around the sample. The word "CHINA" was displayed using this method (Fig. 4c–f). The pre-stored information in the micropillar array can also be read by using 532 nm laser irradiation, the PEG-DA hydrogel micropillar emitted bright red light and represented as "1", nearly no fluorescence could be observed from the methacrylate-based micropillars and represented as "0" (Fig. 4b). The other letters of the alphabet can be demodulated similarly such as the word "JLU", which is a short name of Jilin University (Fig. 4g–j; Movie S5, Supporting Information), and the reproducible of the binary codes and decodes was excellent (Fig. S12–14, Supporting Information). These micropillar arrays can also be used to pass a hidden password, a five bit password was hid in a 5  $\times$  5 micropillar array, the password of "52134" can be read by using water or using 532 nm laser irradiation (Fig. 4k–n).

Using this two-steps FsLDW method and the concept of combination of active and inert materials, we also fabricated a joint-like cantilever microstructure. Joints are the connecting points of animal bones, which are very important in the realization of various movements. In the joints, muscle contraction drives bone to achieve various forms of function such as flexion and extension, rotation and circumduction. In recent years, the joint structure is widely used in bionic machine such as intelligent robot, artificial limbs,

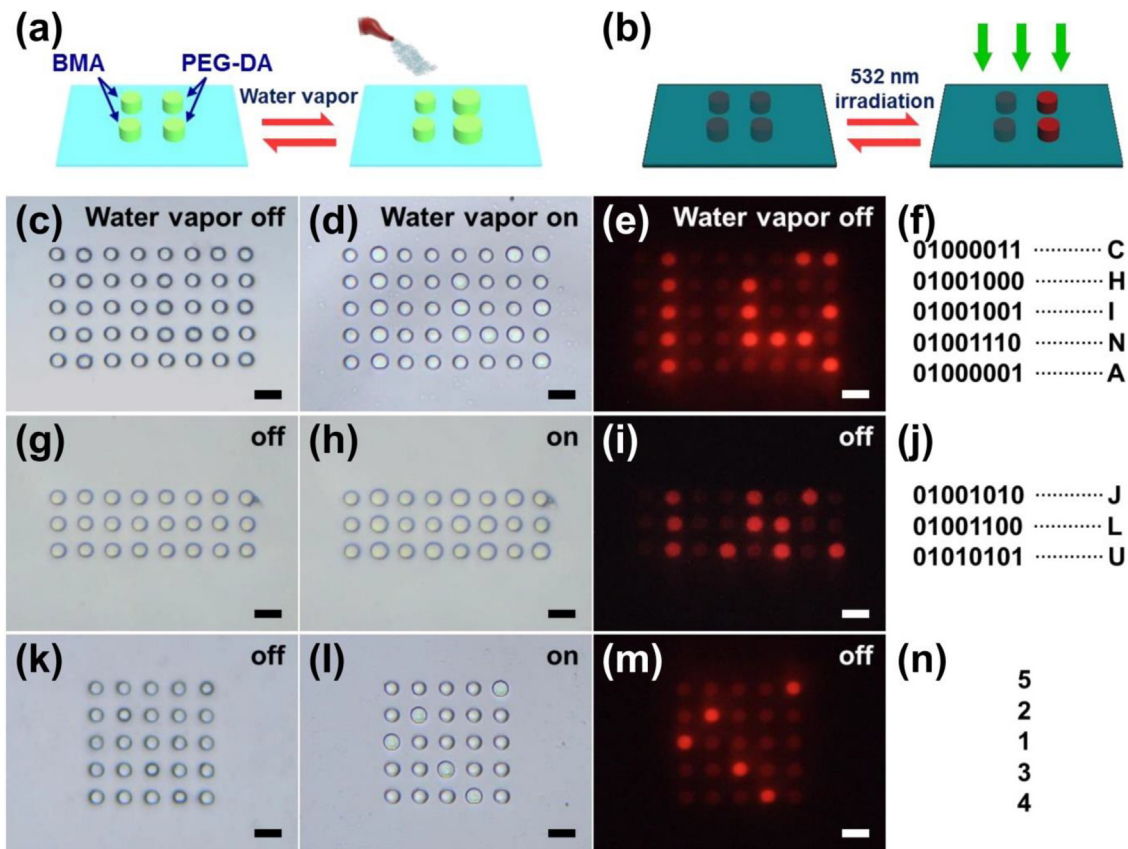


**Fig. 4.** (a)–(b) Schematic of the micropillar array which can be used for data encryption storage and password transmission, the pre-stored information could be read by (a) applying water vapor or (b) irradiating under 532 nm. The word (c)–(f) "CHINA" and (g)–(j) "JLU" were pre-stored and displayed using micropillar array. (k)–(n) A five bit password of "52134" was hid in a 5 × 5 micropillar array. Scale bar: 10 μm. Conditions: T = 20 ± 0.5 °C, RH ≈ 20% when water vapor was off and RH ≈ 100% when water vapor was on.

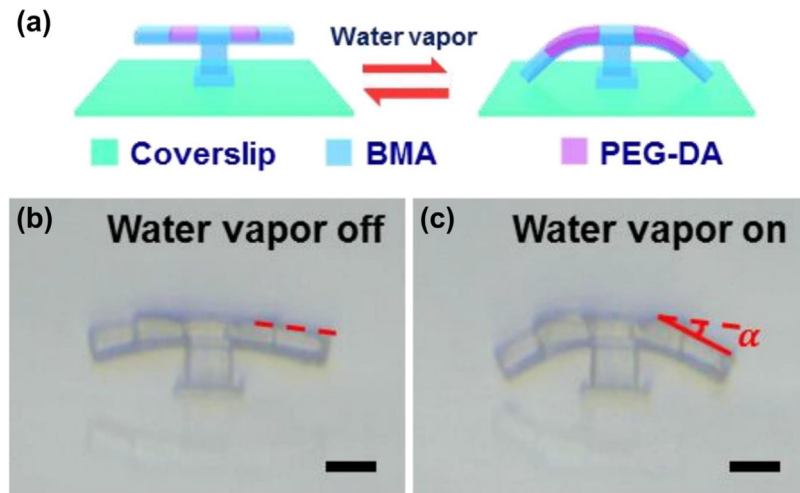


**Fig. 5.** (a) The local directional bending of the cantilever microstructure simulated the bending movement of joint. The cantilever of the joint-like microstructure was (b) almost horizontal after fabrication and (c) bent downward when applying water vapor. Scale bar: 10 μm. Conditions: T = 20 ± 0.5 °C, RH ≈ 20% when water vapor was off and RH ≈ 100% when water vapor was on.

space exploration, remote operation, and machine insect. The fabricated joint-like cantilever microstructure can achieve the function of flexion and extension as joint. The inert methacrylate-based cantilever main structure with grooves was fabricated first and then the active PEG-DA structures were fabricated in the grooves, the obtained joint-like cantilever microstructures could be driven when the RH increased to achieve the directional bending of the partial structure (Fig. 5a). A methacrylate-based cantilever main

structure with grooves of 10 μm × 8 μm × 3 μm was designed, this part have no response to the change of humidity, can serve as "skeleton". After fabricating the PEG-DA hydrogel in these grooves, when the RH increased the PEG-DA part swelled and drove the cantilever structure to bend at the groove positions, these PEG-DA hydrogel parts acted as "muscles". The reversible swell and shrink of "muscles" drive the bending of "bones" (Movie S6; Fig. S15, Supporting Information). The side-view images of the joint-like

micro-structure were showed in Fig. 5b–c, the cantilever structure was almost horizontal after fabrication (Fig. 5b) and when applying water vapor on it, the cantilever structure bent downward at the PEG-DA position (Fig. 5c), the bending angle  $\alpha$  was approximately  $20^\circ$ . We thought that the bending angle can be increased by adjusting the size of the groove precisely.

#### 4. Conclusions

In summary, a kind of humidity response PEG-DA hydrogel microstructure was fabricated by 3D printing FsLDW, which can swell and change volume when driving by humidity. The swelling ability of the PEG-DA microstructure could be adjusted by changing the crosslinking density of voxels during the fabrication. Using the optimized conditions, controllable hydrogel nano-interconnected networks were fabricated which could achieve the interconnection of discrete microstructures. Also stomata-like hydrogel microstructures were fabricated to mimic the open and close of the stomata in plant leaves. Based on the advantages of 3D printing, active PEG-DA hydrogel and inert methacrylate-based material could be combined using a two-steps fabrication method. The function of data encryption storage and password transmission could be achieved by a combined micropillar arrays. A joint-like cantilever microstructure which can directional bend for  $20^\circ$  was presented to simulate the bending movement of joint. The reproducible and endurance properties of the PEG-DA hydrogel microstructures were good under the humidity-driven for several thousand cycles. We believe that this kind of humidity response PEG-DA hydrogel microstructures will be applied to broader applications such as sensors, actuators or construction of soft robots.

#### Acknowledgment

This work was supported by the National Natural Science Foundation of China under Grant Nos 61435005, 51335008, 61590930, 51373064 and 61378053.

#### Appendix A. Supplementary data

Supplementary data associated with this article can be found, in the online version, at <https://doi.org/10.1016/j.snb.2017.12.053>.

#### References

- [1] S.-H. Lee, T.H. Kim, M.D. Lima, R.H. Baughman, S.J. Kim, Biothermal sensing of a torsional artificial muscle, *Nanoscale* 8 (2016) 3248–3253.
- [2] T.Y. Yu, Q. Wang, D.S. Johnson, M.D. Wang, C.K. Ober, Functional hydrogel surfaces: binding kinesin-based molecular motor proteins to selected patterned sites, *Adv. Funct. Mater.* 15 (2005) 1303–1309.
- [3] D. Morales, E. Palley, M.D. Dickey, O.D. Velev, Electro-actuated hydrogel walkers with dual responsive legs, *Soft Matter* 10 (2014) 1337–1348.
- [4] Y.S. Kim, M.J. Liu, Y. Ishida, Y. Ebina, M. Osada, T. Sasaki, T. Hikima, M. Takata, T. Aida, Thermoresponsive actuation enabled by permittivity switching in an electrostatically anisotropic hydrogel, *Nat. Mater.* 14 (2015) 1002–1007.
- [5] C. Lv, H. Xia, Q. Shi, G. Wang, Y.-S. Wang, Q.-D. Chen, Y.-L. Zhang, L.-Q. Liu, H.-B. Sun, Sensitive humidity-driven actuator based on photopolymerizable PEG-DA films, *Adv. Mater. Interfaces* 4 (2017) 1601002.
- [6] K.-U. Jeong, J.-H. Jang, D.-Y. Kim, C. Nah, J.H. Lee, M.-H. Lee, H.-J. Sun, C.-L. Wang, S.Z.D. Cheng, E.L. Thomas, Three-dimensional actuators transformed from the programmed two-dimensional structures via bending, twisting and folding mechanisms, *J. Mater. Chem.* 21 (2011) 6824–6830.
- [7] A.V. Salvekar, W.M. Huang, R. Xiao, Y.S. Wong, S.S. Venkatraman, K.H. Tay, Z.X. Shen, Water-responsive shape recovery induced buckling in biodegradable photo-cross-linked poly(ethylene glycol) (PEG) hydrogel, *Acc. Chem. Res.* 50 (2017) 141–150.
- [8] T.S. Shim, S.-H. Kim, C.-J. Heo, H.C. Jeon, S.-M. Yang, Controlled origami folding of hydrogel bilayers with sustained reversibility for robust microcarriers, *Angew. Chem. Int. Ed.* 51 (2012) 1420–1423.
- [9] L.D. Zhang, S. Chizhik, Y.Z. Wen, P. Naumov, Directed motility of hygroresponsive biomimetic actuators, *Adv. Funct. Mater.* 26 (2016) 1040–1053.
- [10] M.M. Song, M.J. Cheng, M. Xiao, L.N. Zhang, G.N. Ju, F. Shi, Biomimicking of a swim bladder and its application as a mini-generator, *Adv. Mater.* 29 (2017) 1603312.
- [11] A.W. Hauser, A.A. Evans, J.-H. Na, R.C. Hayward, Photothermally reprogrammable buckling of nanocomposite gel sheets, *Angew. Chem. Int. Ed.* 54 (2015) 5434–5437.
- [12] M. Xiao, C. Jiang, F. Shi, Design of a UV-responsive microactuator on a smart device for light-induced ON-OFF-ON motion, *NPG Asia Mater.* 6 (2014) e128.
- [13] K. Iwaso, Y. Takashima, A. Harada, Fast response dry-type artificial molecular muscles with [c2] daisy chains, *Nat. Chem.* 8 (2016) 625–632.
- [14] D. Morales, B. Bharti, M.D. Dickey, O.D. Velev, Bending of responsive hydrogel sheets guided by field assembled microparticle endoskeleton structures, *Small* 12 (2016) 2283–2290.
- [15] C.J. Yu, Z. Duan, P.X. Yuan, Y.H. Li, Y.W. Su, X. Zhang, Y.P. Pan, L.L. Dai, R.G. Nuzzo, Y.G. Huang, H.Q. Jiang, J.A. Rogers, Electronically programmable, reversible shape change in two- and three-dimensional hydrogel structures, *Adv. Mater.* 25 (2013) 1541–1546.
- [16] J.P. Ge, J. Goebel, L. He, Z.D. Lu, Y.D. Yin, Rewritable photonic paper with hygroscopic salt solution as ink, *Adv. Mater.* 21 (2009) 1–6.
- [17] A. Sidorenko, T. Krupenkin, A. Taylor, P. Fratzl, J. Aizenberg, Reversible switching of hydrogel-actuated nanostructures into complex micropatterns, *Science* 315 (2007) 487–490.
- [18] L.D. Zhang, H.R. Liang, J. Jacob, P. Naumov, Photogated humidity-driven motility, *Nat. Commun.* 6 (2015) 7429.
- [19] J.E. Stumpel, E.R. Gil, A.B. Spoelstra, C.W.M. Bastiaansen, D.J. Broer, A.P.H.J. Schenning, Stimuli-responsive materials based on interpenetrating polymer liquid crystal hydrogels, *Adv. Funct. Mater.* 25 (2015) 3314–3320.
- [20] R.M. Erb, J.S. Sander, R. Grisch, A.R. Studart, Self-shaping composites with programmable bioinspired microstructures, *Nat. Commun.* 4 (2013) 1712.
- [21] A.S. Gladman, E.A. Matsumoto, R.G. Nuzzo, L. Mahadevan, J.A. Lewis, Biomimetic 4D printing, *Nat. Mater.* 15 (2016) 413–418.
- [22] M.M. Ma, L. Guo, D.G. Anderson, R. Langer, Bio-inspired polymer composite actuator and generator driven by water gradients, *Science* 339 (2013) 186–189.
- [23] P. Fratzl, F.G. Barth, Biomaterial systems for mechanosensing and actuation, *Nature* 462 (2009) 442–448.
- [24] C. Dawson, J.F.V. Vincent, A.-M. Rocca, How pine cones open, *Nature* 390 (1997) 668.
- [25] R. Elbaum, L. Zaltzman, I. Burgert, P. Fratzl, The role of wheat awns in the seed dispersal unit, *Science* 316 (2007) 884–886.
- [26] O.L. Large, R. Lösch, E.-D. Schulze, L. Kappen, Responses of stomata to changes in humidity, *Planta* 100 (1971) 76–86.
- [27] H. Kim, S.-J. Lee, Stomata-inspired membrane produced through photopolymerization patterning, *Adv. Funct. Mater.* 25 (2015) 4496–4505.
- [28] H. Kim, S.-J. Lee, Fabrication of triple-parted stomata-inspired membrane with stimulus-responsive functions, *Sci. Rep.* 6 (2016) 21258.
- [29] D.J. Beebe, J.S. Moore, J.M. Bauer, Q. Yu, R.H. Liu, C. Devadoss, B.-H. Jo, Functional hydrogel structures for autonomous flow control inside microfluidic channels, *Nature* 404 (2000) 588–590.
- [30] A.K. Agarwal, S.S. Sridharamurthy, D.J. Beebe, H.R. Jiang, Programmable autonomous micromixers and micropumps, *J. Micro-electromech. Syst.* 14 (2005) 1409–1421.
- [31] B. Kaehr, J.B. Shear, Multiphoton fabrication of chemically responsive protein hydrogels for microactuation, *PNAS* 105 (2008) 8850–8854.
- [32] C. Lv, H. Xia, W. Guan, Y.-L. Sun, Z.-N. Tian, T. Jiang, Y.-S. Wang, Y.-L. Zhang, Q.-D. Chen, K. Ariga, Y.-D. Yu, H.-B. Sun, Integrated optofluidic-microfluidic twin channels, toward diverse application of lab-on-a-chip systems, *Sci. Rep.* 6 (2016) 19801.
- [33] Y.-L. Sun, W.-F. Dong, L.-G. Niu, T. Jiang, D.-X. Liu, L. Zhang, Y.-S. Wang, Q.-D. Chen, D.-P. Kim, H.-B. Sun, Protein-based soft micro-optics fabricated by femtosecond laser direct writing, *Light: Sci. Appl.* 3 (2014) e129.
- [34] D. Serien, S. Takeuchi, Fabrication of submicron proteinaceous structures by direct laser writing, *Appl. Phys. Lett.* 107 (2015) 013702.
- [35] D. Wu, J. Xu, L.-G. Niu, S.-Z. Wu, K. Midorikawa, K. Sugioka, In-channel integration of designable microoptical devices using flat scaffold-supported femtosecond-laser microfabrication for coupling-free optofluidic cell counting, *Light: Sci. Appl.* 4 (2015) e228.
- [36] W. Xiong, Y.S. Zhou, X.N. He, Y. Gao, M. Mahjouri-Samani, L. Jiang, T. Baldacchini, Y.F. Lu, Simultaneous additive and subtractive three-dimensional nanofabrication using integrated two-photon polymerization and multiphoton ablation, *Light: Sci. Appl.* 1 (2012) e6.
- [37] M. Malinauskas, A. Žukauskas, S. Hasegawa, Y. Hayasaki, V. Mizeikis, R. Buividas, S. Juodkazis, Ultrafast laser processing of materials, from science to industry, *Light: Sci. Appl.* 5 (2016) e16133.
- [38] Y.-L. Sun, S.-M. Sun, P. Wang, W.-F. Dong, L. Zhang, B.-B. Xu, Q.-D. Chen, L.-M. Tong, H.-B. Sun, Customization of protein single nanowires for optical biosensing, *Small* 11 (2015) 2869–2876.
- [39] H. Xia, J. Wang, Y. Tian, Q.-D. Chen, X.-B. Du, Y.-L. Zhang, Y. He, H.-B. Sun, Ferrofluids for fabrication of remotely controllable micro-nanomachines by two-photon polymerization, *Adv. Mater.* 22 (2010) 3204–3207.
- [40] R. Krini, C.W. Ha, P. Prabhakaran, H.E. Mard, D.-Y. Yang, R. Zentel, K.-S. Lee, Photosensitive functionalized surface-modified quantum dots for polymeric structures via two-photon-initiated polymerization technique, *Macromol. Rapid Commun.* 36 (2015) 1108–1114.

- [41] Q. Sun, K. Ueno, H. Misawa, In situ investigation of the shrinkage of photopolymerized micro/nanostructures: the effect of the drying process, *Opt. Lett.* 37 (2012) 710–712.
- [42] C.L. Lay, M.R. Lee, H.K. Lee, I.Y. Phang, X.Y. Ling, Transformative two-dimensional array configurations by geo-metrical shape-shifting protein microstructures, *ACS Nano* 9 (2015) 9708–9717.
- [43] M.R. Lee, I.Y. Phang, Y. Cui, Y.H. Lee, X.Y. Ling, Shape-shifting 3D protein microstructures with programmable directionality via quantitative nanoscale stiffness modulation, *Small* 11 (2015) 740–748.
- [44] Y.B. Wu, S. Joseph, N.R. Aluru, Effect of cross-linking on the diffusion of water ions, and small molecules in hydrogels, *J. Phys. Chem. B* 113 (2009) 3512–3520.
- [45] F. Zhao, L.X. Wang, Y. Zhao, L.T. Qu, L.M. Dai, Graphene oxide nanoribbon assembly toward moisture powered information storage, *Adv. Mater.* 29 (2017) 1604972.

## Biographies

**Chao Lv** received her Ph.D. in Electronic Science and Engineering from Jilin University in 2017. Her research interests include stimulus-responsive hydrogels and soft actuators.

**Xiang-Chao Sun** is currently a Master student at Jilin University, China. His research interest lies in humidity responsive micro-nanoactuators.

**Hong Xia** received her Ph.D. degree in Chemistry from Jilin University, China, in 2006. She is currently a full professor at Jilin University. Her research interests include intelligent materials, stimulus-responsive actuators and laser microfabrication.

**Yan-Hao Yu** received his Ph.D. degree in 2016 at Jilin University, China. His research interest focuses on laser microfabrication.

**Gong Wang** is pursuing his Ph.D. at Jilin University, China. His research interests lie in the field of piezoelectric polymer, controlled deformations of soft actuators, energy device for energy conversion.

**Xiao-Wen Cao** is pursuing his Ph.D. at Jilin University, China. His research interests include theory of the interaction of femtosecond laser and material and fabrication of micro-nano structure.

**Shun-Xin Li** is pursuing her Ph.D. at Jilin University, China. Her research interests include organic crystal and nanofabrication.

**Ying-Shuai Wang** received his Ph.D. in Electronic Science and Engineering from Jilin University in 2017. His research interests lie in the field of micro motor and application of nanocomposites.

**Qi-Dai Chen** received his Ph.D. in Institute of Physics from The Chinese Academy of Sciences, China, in 2004. He is currently a full professor at Jilin University. His research interests include laser microfabrication, ultrafast laser spectroscopy, photochemistry and photophysics.

**Yu-De Yu** graduated from the Department of Physics, University of Science and Technology of China, Hefei, China, in 1977. From 1977 to 2003, he worked in the Institute of Physics, Chinese Academy of Sciences (CAS), Beijing, China, and his research field focused on crystal structure analysis by X-ray diffraction, new material exploration, single crystal growth, and material science research under microgravity condition. During 1987–1989, he did research work on neutron scattering at Institute fuer Kristallographie, University of Munch, Germany, as a Visiting Scholar. In 2003, he transferred to Institute of Semiconductors, CAS. His present interests include Si-based photonics and material science research under microgravity condition.

**Hong-Bo Sun** received the B.S. and the Ph.D. degrees in electronics from Jilin University, China, in 1992 and 1996, respectively. He worked as a postdoctoral researcher in Satellite Venture Business Laboratory, the University of Tokushima, Japan, from 1996 to 2000, and then as an assistant professor in Department of Applied Physics, Osaka University, Japan. In 2004, he was promoted as a full professor (Changjiang Scholar) in Jilin University, and since 2017 he has been working in Tsinghua University, China. His research interests have been focused on ultrafast optoelectronics, particularly on laser nanofabrication and ultrafast spectroscopy: Fabrication of various micro-optical, microelectronical, micromechanical, micro-optoelectronic, microfluidic components and their integrated systems at nanoscale, and exploring ultrafast dynamics of photons, electrons, phonons, and surface plasmons in solar cells, organic light-emitting devices and low-dimensional quantum systems at femtosecond timescale. So far, he has published over 350 scientific papers in the above fields, which have been cited for more than 12000 times according to ISI search report. He is currently the topical editor of Optics Letters (OSA), Light: Science and Applications (Nature Publishing Group), Chinese Science Bulletin (Springer), and editorial advisory board member of Nanoscale (RSC) and Display and Imaging (Old City Publishing).